

## Investigations on exponential lifetime measurements for fluorescence thermometry

V. C. Fericola, L. Rosso, R. Galleano, T. Sun, Z. Y. Zhang, and K. T. V. Grattan

Citation: [Review of Scientific Instruments](#) **71**, 2938 (2000); doi: 10.1063/1.1150714

View online: <http://dx.doi.org/10.1063/1.1150714>

View Table of Contents: <http://scitation.aip.org/content/aip/journal/rsi/71/7?ver=pdfcov>

Published by the [AIP Publishing](#)

---

### Articles you may be interested in

[Er 3+ -doped BaTiO 3 nanocrystals for thermometry: Influence of nanoenvironment on the sensitivity of a fluorescence based temperature sensor](#)

Appl. Phys. Lett. **84**, 4753 (2004); 10.1063/1.1760882

[Fiber optic sensor for dual measurement of temperature and strain using a combined fluorescence lifetime decay and fiber Bragg grating technique](#)

Rev. Sci. Instrum. **72**, 3186 (2001); 10.1063/1.1372171

[Modeling the fluorescent lifetime of Y 2 O 3 :Eu](#)

Appl. Phys. Lett. **72**, 2663 (1998); 10.1063/1.121091

[Application of singular value decomposition in average temperature measurement using fluorescence decay techniques](#)

Rev. Sci. Instrum. **69**, 1716 (1998); 10.1063/1.1148831

[Fiber optic thermometry based on Cr-fluorescence in olivine crystals](#)

Rev. Sci. Instrum. **68**, 2418 (1997); 10.1063/1.1148126

---



**OXFORD**  
INSTRUMENTS  
*The Business of Science®*

**'On the way to a  
graphene spin field effect transistor'**  
by Prof. Barbaros and the Özyilmaz Group at National University of Singapore

**Download a FREE application note**

# Investigations on exponential lifetime measurements for fluorescence thermometry

V. C. Fericola,<sup>a)</sup> L. Rosso, and R. Galleano  
*Istituto di Metrologia "G. Colonnelli," CNR, Torino, Italy*

T. Sun, Z. Y. Zhang, and K. T. V. Grattan<sup>b)</sup>  
*City University, London EC1V0MB, United Kingdom*

(Received 25 January 2000; accepted for publication 15 March 2000)

Lifetime-based methods have been, on the whole, one of the most successful schemes for fiber optic temperature sensing, using fluorescent materials whose response is intensity independent. Several approaches for determining the fluorescence lifetime, and with that the measurand, have been investigated. An experimental comparison of direct and indirect measurement methods, i.e., involving actual signals from representative optical media instead of simply using Monte Carlo simulations, has been carried out. Direct fitting methods, including Marquardt, log-fit and Prony, were used to estimate the fluorescence lifetime of a  $\text{Cr}^{3+}$ :YAG-based sensor system and the results were compared. An agreement to better than 0.5% between Marquardt and log-fit algorithms and an agreement of about 1.5% between Marquardt and Prony approaches was found. Thus, a temperature reproducibility, of 0.5 and 1.2 °C, respectively, can be obtained with the  $\text{Cr}^{3+}$ :YAG sensor system. An indirect measurement approach based on a phase-locked (analog-to-digital signal processor) (A-DSP) was also tested. It was found that when the A-DSP output is used to estimate the lifetime, it performs only slightly better than using direct fitting methods. On the contrary, when the whole A-DSP sensor system was directly calibrated against temperature, the measurement accuracy improves by at least a factor of 10. © 2000 American Institute of Physics.  
[S0034-6748(00)01807-4]

## I. INTRODUCTION

Luminescence-based methods of sensing temperature and strain have proved simple and versatile, and a range of different fiber-optic based sensor probes has been developed in recent years. Of these, fluorescence techniques show considerable promise, with the major advantage of being intensity independent when the decay time of the luminescence is monitored. This has been, in fact, the predominant technique used in a range of, for example, temperature sensors.<sup>1</sup> The familiar advantages of the use of optical and fiber-based techniques apply equally to these approaches.

A crucial factor in the calibration, use, and reproducibility of such sensors is the interpretation of the decay time information obtained from the sensor material itself. In practice, in such sensor devices, a range of factors may influence the interpretation of the decay time information, leading to measurement errors. These include any sources of noise in the system and in the circuits used, stray illumination at wavelengths which are not those of the fluorescence signal, errors in the signal processing approach, and any approximations employed. A key factor in this is the choice of algorithm used to interpret the signal at the photodetector and a number of different techniques have been used and reported in the literature.<sup>2-5</sup> A comprehensive review of exponential decay measurements methods, both in the time and in the

frequency domain, has recently been discussed.<sup>3</sup>

The purpose of the present work is to undertake a quantitative assessment of a range of such approaches, using the same type of representative sensor probe, in this case for temperature monitoring. The prime motivation of the study is to cross-compare the results of lifetime measurements, using different time-domain methods. An experimental comparison, i.e., not involving Monte Carlo simulations, between direct and indirect measurement methods using the actual signals received from optical media commonly used as temperature sensors, was carried out. The fluorescence lifetime of a Cr:YAG crystal, a representative temperature sensing material, was determined by means of direct fitting of three different least square approximation algorithms to the exponential decay data, i.e., Marquardt nonlinear fitting, log-linear fitting, and noniterative Prony's method. The results were also compared with those from a calibrated Cr:YAG temperature sensing system, based on an analog-to-digital signal processing (A-DSP) approach, which acts as a lifetime-to-period converter and whose output is linearly dependent on the measured lifetime.<sup>4</sup>

## II. EXPERIMENTAL ARRANGEMENT

### A. Temperature probe

A  $\text{Cr}^{3+}$ :YAG crystal, cylindrical shaped, 5 mm long and 3 mm in diameter, was used in the experiment as a temperature sensing element.  $\text{Cr}^{3+}$ :YAG exhibits absorption in a wide band centered at about 600 nm and fluorescent emis-

<sup>a)</sup>Author to whom correspondence should be addressed; electronic mail: v.fericola@imgc.to.cnr.it

<sup>b)</sup>Electronic mail: k.t.v.grattan@city.ac.uk

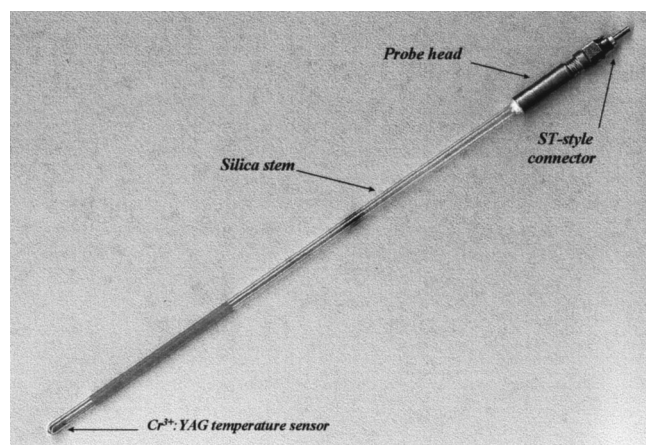


FIG. 1. The  $\text{Cr}^{3+}$ :YAG fiber optic temperature probe assembled in a silica stem.

sion near 687 nm (the  $R$  lines) with a broadband tail up to 800 nm.<sup>6</sup> The temperature probe was assembled by placing the crystal on the bottom of a silica sheath (300 mm in length and 6 mm o.d.), and guiding a multimode silica optical fiber toward the bottom of the sheath by means of a coaxial capillary tube. The optical fiber was butt-coupled to the crystal and terminated at the other end with a standard ST connector held by the probe head (Fig. 1). With this configuration, it can be detached from the optical fiber extension cable enabling an easier handling of the probe itself. The probe head can be removed from the thermometer stem and the probe disassembled so that the sensing material can be replaced, if required.

### 1. Annealing of the temperature sensor

In the lifetime measurement comparison based on a temperature sensor, the annealing of the sensor element is necessary to remove one of the major sources of error arising from a lack of reproducibility in the calibration response of the sensor itself.<sup>7</sup> As all experiments were based on the actual response from a fluorescent material, the  $\text{Cr}^{3+}$ :YAG temperature sensor was annealed, in order to achieve a good temperature stability of the calibration curve as had been shown in previous work. The sensor was repeatedly exposed at 400 °C in an oven and, at given time intervals, withdrawn from it and introduced into an ice bath. Under this condition (at 0 °C) the output of the phase-locked A-DSP, that is the modulation period  $T$ , was recorded. These high-temperature excursions were repeated until the difference between the  $T$  values was lower than 14  $\mu\text{s}$ , corresponding to a temperature difference of about 0.05 °C. The  $T$  values with their associated standard uncertainties are depicted in Fig. 2 as a function of the annealing time. Figure 2 highlights that by using the  $\text{Cr}^{3+}$ :YAG sensor, a high temperature stability can be achieved.

### B. Optical–electrical setup

A 635 nm laser diode (LD) was used for excitation; the LD radiation was launched into one port of a bidirectional 1×2 fiber optic coupler by means of a gradient index lens and delivered to the crystal. The fluorescence response from

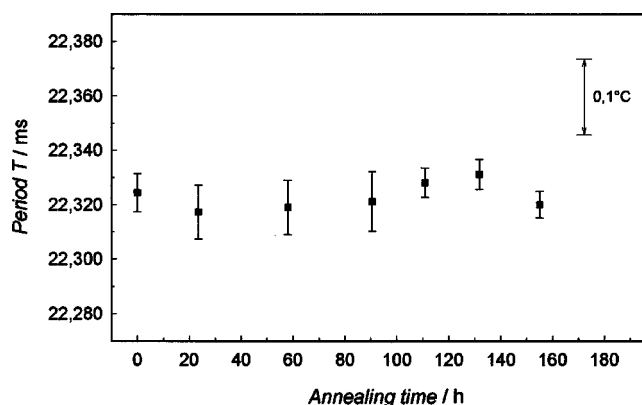


FIG. 2. Temperature stability at 0 °C of the Cr:YAG fiber optic sensor after repeated excursions to 400 °C.

the crystal, passing through the same fiber, was conveyed into the other port of the coupler. Due to the back reflections at the many optical interfaces, the fluorescence signal could have been buried under the intense excitation signal. Thus, in order to avoid a saturation of the detection stage and to enable the fluorescence response to be detected exclusively, a bandpass interference filter ( $F$ ) with peak transmission at 694 nm (Corion S10-694) was placed before the Si pin photodetector (PD). However, even after optical filtering, some residual excitation light leaks into the detection stage and may cause a decay time measurement error. To overcome this problem, the fluorescence response was exclusively monitored during the decaying phase, when the excitation light was turned off. Figure 3 shows the diagram of the lifetime measurement setup in the two configurations, used for direct (1) and indirect (2) measurements, respectively.

### C. Lifetime measurements methods

Different methods, both direct and indirect, were applied to determine the lifetime value  $\tau$ . With the direct methods, the fluorescence lifetime was obtained, at each temperature, by directly acquiring the output of the photodetector with a digital sampling oscilloscope (DSO). The LD was modulated by a periodic rectangular signal from a wave form generator

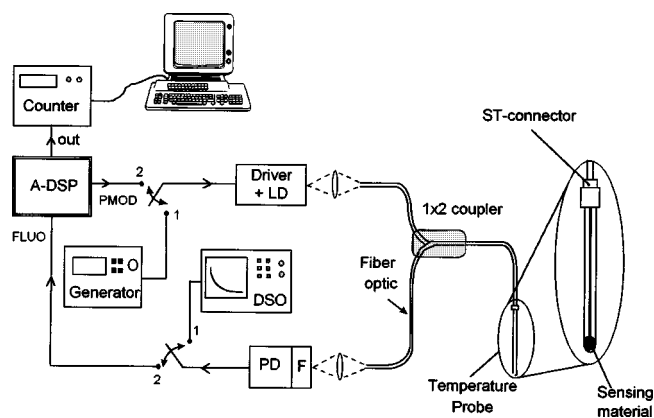


FIG. 3. Block diagram of the lifetime measurement system; switch in position 1: the decay data are directly acquired by the DSO to determine  $\tau$ ; switch in position 2: the system operation is based on an A-DSP module whose output is a modulation period  $T$ , and is measured by a counter. (For an explanation of the symbols, please refers to text.)

(switch position 1 in Fig. 3) and the acquisition of the fluorescence signal started as soon as the LD was turned off. A set of fluorescence decay curves were collected, at different temperatures, and the lifetime values evaluated.

An indirect method for the lifetime measurement was also used. This method, based on a phase-locked A-DSP,<sup>4</sup> allows the determination of  $\tau$  by measuring the output modulation period  $T$  which is, in turn, correlated to the fluorescence lifetime. In fact the A-DSP module converts the fluorescence response from the probe into a digital signal of period  $T$  (switch position 2 in Fig. 3). Its closed-loop operation is such that the modulation period  $T$  is automatically adjusted to match the measured lifetime  $\tau$  in a directly proportional way. As a result, the lifetime is indirectly obtained from a measurement of  $T$  by means of a frequency counter. More details about the “phase locked techniques” can be found in the publications of Grattan and Zhang,<sup>1</sup> and Fornicola and Crovini.<sup>4</sup>

### III. DATA PROCESSING AND CALIBRATION

#### A. Direct determination of lifetime

The fluorescence lifetime  $\tau$  of the sensor was directly determined by acquiring the experimental decay intensity with a DSO and, then fitting the data to the well-known function

$$V(t) = A \exp(-t/\tau) + B, \quad (1)$$

where  $A$  and  $B$  are the initial fluorescence amplitude and the baseline offset, respectively.

Different fitting methods of the decay curve sample data were compared. The fluorescence lifetime was estimated using a Marquardt nonlinear least squares approximation algorithm, a log-fit linear least square algorithm, and a noniterative Prony-correlation method.

#### 1. Marquardt method

The Marquardt algorithm combines the best features of the gradient search with the method of linearizing the fitting function. In this algorithm, the first step is to introduce the fitting function and then to define a  $\chi^2$  function by using Taylor's expansion. At this point, the gradient search is used

for minimizing the  $\chi^2$  function. After the parameters to be estimated have been initialized, the method looks for the minimum of the function in the direction of the gradient. Marquardt also introduced a  $\lambda$  parameter, which is used to set the interval in which the  $\chi^2$  function, along the gradient line, will be evaluated.<sup>8</sup>

Previous work<sup>2,9</sup> based on Monte Carlo simulations has shown that for a fixed rms noise amplitude, the lifetime estimation error is a function of  $\beta$  (the ratio between the observation window  $\Delta T$  and the lifetime  $\tau$ ). For the Marquardt algorithm, the error is minimum for  $\beta > 4$ . In this work data were processed in a  $5\text{-}\tau$  observation window.

#### 2. Log-fit method

Another estimation algorithm, termed here the log-fit, was used to estimate the fluorescence lifetime. It consists of applying the linear least-squares approximation to the logarithm of the fitting function, given by Eq. (1), after the subtraction of the baseline offset  $B$ ; thus resulting in

$$\ln(V(t) - B) = (-t/\tau) + \ln(A). \quad (2)$$

Only two parameters  $A$  and  $\tau$  were thus estimated. With regard to the baseline offset, introduced in Eq. (2), it was determined in one of two different ways: (a) as the asymptotical value of the decay signal  $V(t)$ , averaged over a  $1\text{-}\tau$  window, for  $t > 6\tau$ ; (b) as the value given by the previous Marquardt fitting. The two estimates agreed better than 0.1%, i.e., to within their standard uncertainty.

As far as the log-fit algorithm is concerned, in order to minimize the lifetime estimation error,  $\beta$  is kept equal to 1.3.<sup>9</sup>

#### 3. Prony method

Prony's method is a noniteration algorithm for an approximation of a sum of exponentials. To fit the three-parameter model expressed in Eq. (1),  $(N - \Delta j - \Delta N)$  linear equations are found from the  $N$  samples

$$(f_j - f_{j+\Delta j})\alpha + (f_{j+\Delta N} - f_{j+\Delta j+\Delta N}) = 0, \quad (3)$$

where  $\Delta j$  is the differential space index, and  $\Delta N$  the sample spacing index.

The estimation of the lifetime will be given by

TABLE I. Lifetimes and associated standard uncertainties, estimated at different temperatures, with Marquardt, log-fit, and Prony algorithm, respectively.

$\theta/^\circ\text{C}$	Marquardt		Log-fit		Prony	
	$\tau/\text{s}$	$u_\tau/\text{s}$	$\tau/\text{s}$	$u_\tau/\text{s}$	$\tau/\text{s}$	$u_\tau/\text{s}$
0.00	2.262E-03	1.80E-06	2.254E-03	2.17E-06	2.292E-03	6.42E-06
22.00	1.722E-03	1.25E-06	1.719E-03	1.48E-06	1.748E-03	4.21E-06
49.57	1.235E-03	6.44E-07	1.233E-03	7.46E-07	1.242E-03	2.52E-06
74.40	9.300E-04	5.45E-07	9.257E-04	7.35E-07	9.352E-04	1.75E-06
99.47	7.215E-04	3.08E-07	7.223E-04	3.98E-07	7.206E-04	1.24E-06
124.69	5.711E-04	2.41E-07	5.719E-04	3.04E-07	5.707E-04	7.61E-07
149.91	4.649E-04	2.11E-07	4.652E-04	2.71E-07	4.642E-04	5.67E-07
175.02	3.869E-04	1.78E-07	3.875E-04	2.30E-07	3.858E-04	4.06E-07
200.31	3.272E-04	8.21E-08	3.279E-04	1.13E-07	3.255E-04	2.61E-07
229.83	2.773E-04	8.91E-08	2.781E-04	1.13E-07	2.767E-04	2.34E-07
254.42	2.449E-04	8.06E-08	2.452E-04	9.62E-08	2.443E-04	2.58E-07
274.26	2.238E-04	8.73E-08	2.230E-04	9.69E-08	2.237E-04	2.13E-07
299.27	1.982E-04	7.50E-08	1.982E-04	9.70E-08	1.976E-04	1.45E-07



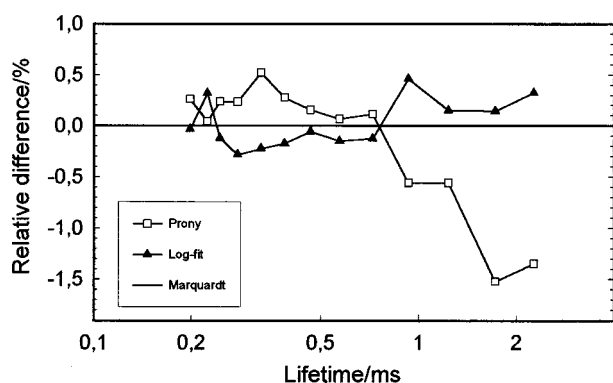


FIG. 4. Percent relative differences among various lifetime estimation methods (Marquardt approach taken as reference).

$$\tau = (\Delta N)(\Delta t) / \ln(-1/\alpha). \quad (4)$$

Basically, there are two ways to approximate  $\alpha$  using Eq. (3), with either superposition or a correlation scheme, of which the correlation scheme is more accurate, and which has been used in this work. In this case, optimum performance can be achieved when  $\beta$  is in the region of 4.5–5.<sup>2</sup>

## B. Comparison of different fitting methods

Table I shows the results obtained when Marquardt, log-fit, and Prony algorithms are used to estimate fluorescence lifetimes, at several temperatures, with their standard uncertainties. Figure 4 shows the relative lifetime differences  $\Delta\tau/\tau$  in percentage terms, between the results obtained using the log-fit, Prony, and Marquardt algorithms (whose estimates are used as reference). The graph points out, in the lifetime range from 0.2 to 2.3 ms (typical of many rare earth fluorescence transitions), an agreement to better than 0.5% between Marquardt and log-fit and an agreement to within 1.5% between the Marquardt and Prony methods. Although the noise-to-error transfer is a little higher than the other two, the execution time of Prony's method is much shorter than that of the other two.<sup>2</sup> As this work deals with an actual optical medium used as temperature sensor, it is worthwhile to express the same estimation agreement in temperature units. Figure 5 indicates the same differences as converted in terms of temperature through the  $\text{Cr}^{3+}:\text{YAG}$  sensitivity curve. A

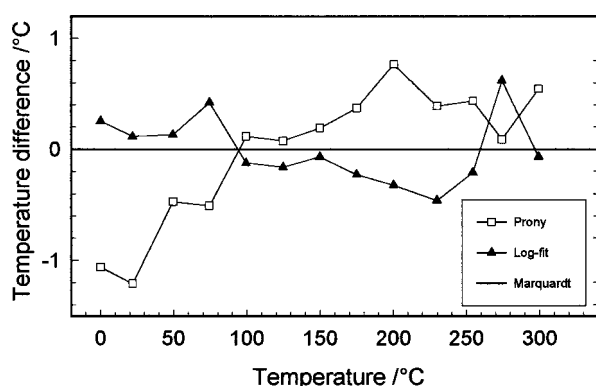


FIG. 5. Temperature differences among the results obtained with various estimation methods (Marquardt approach taken as reference) using a  $\text{Cr}^{3+}:\text{YAG}$  sensor probe.

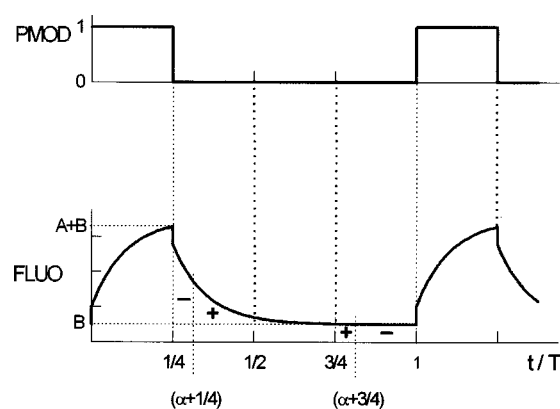


FIG. 6. LD excitation signal (PMOD) and fluorescence response (FLUO) of the temperature sensor.

temperature difference to within 0.5 °C between Marquardt and log-fit and to within 1.2 °C between Marquardt and Prony is found.

## C. Indirect determination of lifetime with an A-DSP sensing system

### 1. Principle of operation

A different approach taken to lifetime measurements was to exploit a phase-locked A-DSP-based system. The LD was modulated by a rectangular signal of period  $T$  (PMOD in Fig. 6) and used to excite the temperature sensing crystal. When the LD is in the “off” state, the fluorescence decay signal (FLUO) is digitally integrated by means of a voltage-to-frequency converter, cascaded to an up-and-down binary counter. The counter switches from the up to the down mode when the signal passes from the area marked “+” to that marked “−.” The integration intervals (of the decay signal) are phase locked to the excitation period  $T$  and are multiple of  $\alpha T$ , where  $\alpha$  is a constant phase shift. The integration sign, for each interval, is determined by use of suitable control logic. The digital output  $N$ , given by the counter, is stored in a latch and then loaded into a 16-bit down counter to generate the PMOD signal. Due to the output logic, the modulation period resulting is equal to  $T = kNt_{\text{clock}}$ , where  $k$  (equal to 16) is a constant of the system and  $t_{\text{clock}}$  is the clock period. For a fixed  $\alpha$ ,  $N$  will change until the system reaches its balanced condition, which corresponds to an integral under the decay curve equal to zero. From this point on, the feedback will keep  $N$  constant and the period  $T$  will track the decay time changes linearly. This is the so-called “locked state.” Because of the A-DSP module characteristics, the output modulation period  $T$ , in the balanced condition, is linear to the corresponding value of  $\tau$ .

### 2. Calibration of the A-DSP sensing system

The output period  $T$  and the lifetime  $\tau$  were independently determined at each temperature and then fitted to the relationship  $T = x(\tau - \tau_0)$ , where  $x$  is a proportionality constant and  $\tau_0$  accounts for the finite electronic time constant of the system. The  $T$  values were measured with the phase-locked A-DSP, at the same experimental temperatures as before, and the corresponding values of  $\tau$  were estimated with

TABLE II.  $T$  vs  $\tau$  calibration of the A-DSP system (with a  $\text{Cr}^{3+}$ :YAG temperature sensor) and associated standard uncertainties.

$\theta/^\circ\text{C}$	A-DSP output		Marquardt	
	$T/\text{s}$	$u_T/\text{s}$	$\tau/\text{s}$	$u_\tau/\text{s}$
0.00	2.22583E-02	8.57E-07	2.262E-03	1.80E-06
22.00	1.67768E-02	5.89E-07	1.722E-03	1.25E-06
49.57	1.19498E-02	5.45E-07	1.235E-03	6.44E-07
74.40	9.0058E-03	3.72E-07	9.300E-04	5.45E-07
99.47	6.95698E-03	2.80E-07	7.215E-04	3.08E-07
124.69	5.51117E-03	1.97E-07	5.711E-04	2.41E-07
149.91	4.47648E-03	1.49E-07	4.649E-04	2.11E-07
175.02	3.72179E-03	1.22E-07	3.869E-04	1.78E-07
200.31	3.15327E-03	1.04E-07	3.272E-04	8.21E-08
229.83	2.66069E-03	7.45E-08	2.773E-04	8.91E-08
254.42	2.33977E-03	5.97E-08	2.449E-04	8.06E-08
274.26	2.12127E-03	6.56E-08	2.238E-04	8.73E-08
299.27	1.89261E-03	6.16E-08	1.982E-04	7.50E-08

the Marquardt least-squared approximation. The results are summarized in Table II, where the Marquardt column is the same as in Table I.

Linear fittings were performed using both ordinary least-squared (OLS) and weighted least-squared (WLS) algorithms to estimate  $x$  and  $\tau_0$  of the calibration curve of the whole measurement chain (A-DSP+PD+PD). The results are collected in Table III.

A comparison between OLS and WLS algorithms (Fig. 7) reveals that WLS gave better results with fitting residuals in the range from 0.1% to 1.2%; OLS fitting residuals are larger and they vary in the range from 0.2% to 2%. Furthermore, with WLS, the straight line slope is also closer to the theoretical value ( $x=9.750$  from Ref. 4). A previous estimate of  $x$  and  $\tau_0$ , from the calibration of the A-DSP module alone, in the range from 200  $\mu\text{s}$  to 2.2 ms, gave  $x'=9.761$  and  $\tau'_0=0.51 \mu\text{s}$ . By comparing these values with those obtained with the present WLS estimates, a good agreement for  $x$  is found; the difference in  $\tau_0$  accounts for the additional electronic time constants due to the LD and the PD.

#### D. Use of the A-DSP as a temperature measurement system

The measurement accuracy can be dramatically improved with a direct calibration of the whole A-DSP-based measurement system. Direct calibration was carried out by measuring the values of the modulation period  $T$  as a function of the temperature. A set of 13 well-known temperatures was generated inside a furnace and the  $\text{Cr}^{3+}$ :YAG sensor system was directly calibrated by comparison with the readings of a Pt-100 platinum resistance thermometer. An ice bath was used for the calibration at 0  $^\circ\text{C}$ .

The upper part of Fig. 8 shows the relation between the

TABLE III. Estimates of  $x$  and  $\tau_0$  obtained with OLS and WLS algorithms and associated standard uncertainties.

Parameters	OLS	WLS
$x$	$9.830 \pm 0.025$	$9.745 \pm 0.025$
$\tau_0/\mu\text{s}$	$9.38 \pm 2.45$	$4.7 \pm 0.8$

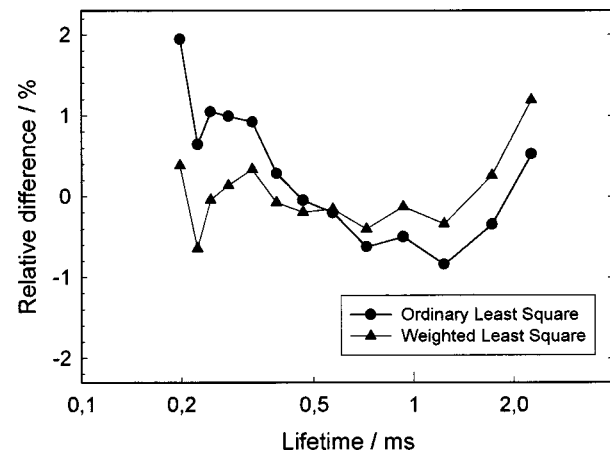


FIG. 7. Relative residuals obtained with OLS and WLS algorithms.

temperature and the corresponding output modulation period  $T$ , in the temperature range 0–300  $^\circ\text{C}$ . The lower part of Fig. 8 indicates the typical measurement uncertainty of the period  $T$  at each experimental point, as converted in temperature unit. A repeatability,  $\Delta\theta$  (at 1- $\sigma$  level), varying from 0.04  $^\circ\text{C}$  at 0  $^\circ\text{C}$  up to 0.12  $^\circ\text{C}$  at 300  $^\circ\text{C}$  resulted.

#### IV. DISCUSSION

Different lifetime measurement methods, both direct and indirect, were investigated over the fluorescence lifetime range 0.2–2.3 ms for potential application of these systems to fiber optic sensors, such as those monitoring temperature and strain. With the direct methods, each lifetime corresponding to a certain temperature was estimated by fitting the experimental decay data to a single exponential function. Three fitting methods, i.e., using the Marquardt, log-fit, and Prony algorithms, were employed to estimate the fluorescence lifetime and then compared. The results showed an agreement to better than 0.5% between Marquardt and log-fit algorithms and an agreement to better than 1.5% between Marquardt and Prony. These results, as converted in terms of temperature, for the optical medium investigated ( $\text{Cr}$ :YAG) indicated a temperature difference of about 0.5  $^\circ\text{C}$  between

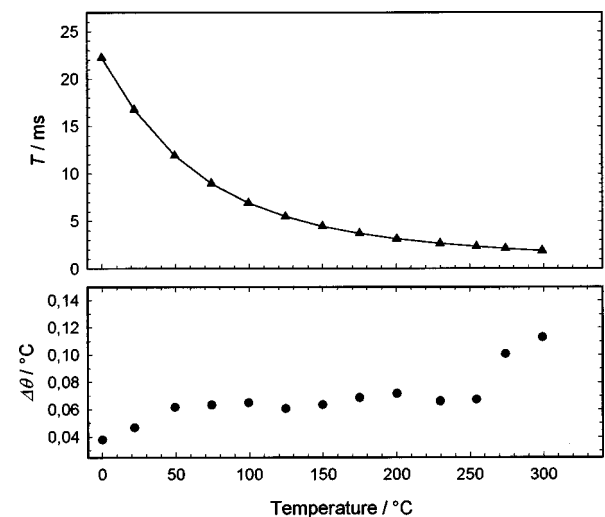


FIG. 8. Calibration curve of the Cr:YAG sensor system (A-DSP output vs temperature) and temperature repeatability at the calibration points.

the Marquardt and log-fit and of about 1.2 °C between the Marquardt and Prony approaches over the temperature range 0–300 °C. From these results, it can be concluded that by using the same experimental apparatus, but different data processing, an equivalent temperature reproducibility can be achieved.

The indirect measurement approach based on the phase-locked A-DSP, whose output period is proportional to the lifetime  $\tau$ , is potentially much more accurate because it is an integration method. The improved signal-to-noise ratio can be clearly seen in the relative uncertainties in  $T$  in Table II, which are more than one order of magnitude lower than the corresponding uncertainties in  $\tau$  obtained from fitting methods. However, when the measurement of  $T$  is used to estimate the lifetime, because of the nonlinearity associated with the calibration curve  $T = x(\tau - \tau_0)$ , the A-DSP performs only slightly better than the direct fitting methods. The temperature measurement accuracy can be significantly improved when the whole A-DSP sensor system is directly calibrated and used as a temperature measurement system. At the same temperatures as before, a good temperature repeatability is achieved, e.g., with the  $\text{Cr}^{3+}$ :YAG sensor system it is in the range from 0.04 to 0.12 °C.

The results of this study have also positive implications for a number of rare earth species, doped into fibers or crystal and garnets, used for temperature and strain sensing. The

lifetimes considered cover those of materials such as  $\text{Yb}^{3+}$ ,  $\text{Nd}^{3+}$ , and  $\text{Er}^{3+}$  for example, and the potential to make more accurate measurements is often very useful. The costs associated with employing such signal processing schemes is reasonable within the typical costs of these type of systems, as they are relatively easy to implement. Thus, the work can be seen to enhance the utility of the rapidly developing field of optical fiber fluorescence-based sensing.

## ACKNOWLEDGMENTS

This work has been carried out within the framework of the British–Italian Collaboration in Research and Higher Education. Partial support from The British Council and Conferenza dei Rettori (CRUI) is kindly acknowledged.

- <sup>1</sup>K. T. V. Grattan and Z. Y. Zhang, *Fiber Optic Fluorescence Thermometry* (Chapman and Hall, London, 1995).
- <sup>2</sup>Z. Y. Zhang, K. T. V. Grattan, Y. L. Hu, A. W. Palmer, and B. T. Meggit, *Rev. Sci. Instrum.* **67**, 2590 (1996).
- <sup>3</sup>A. A. Istratov and O. F. Vyvenko, *Rev. Sci. Instrum.* **70**, 1233 (1999).
- <sup>4</sup>V. C. Farnicola and L. Crovini, *IEEE Trans. Instrum. Meas.* **44**, 447 (1995).
- <sup>5</sup>L. J. Dowell and G. T. Gillies, *Rev. Sci. Instrum.* **59**, 1310 (1998).
- <sup>6</sup>V. C. Farnicola and L. Crovini, *Proc. SPIE* **2070**, 472 (1993).
- <sup>7</sup>Z. Y. Zhang, K. T. V. Grattan, A. W. Palmer, and B. T. Meggit, *Rev. Sci. Instrum.* **69**, 139 (1998).
- <sup>8</sup>D. W. Marquardt, *J. Soc. Ind. Appl. Math.* **11**, 431 (1963).
- <sup>9</sup>L. J. Dowell and G. T. Gillies, *Rev. Sci. Instrum.* **62**, 242 (1990).